Controlled Release

DOI: 10.1002/ange.201303489

Turning Coacervates into Biohybrid Glass: Core/Shell Capsules Formed by Silica Precipitation in Protein/Polysaccharide Scaffolds

Philipp Erni, Gregory Dardelle, Matthew Sillick, Kenneth Wong, Pascal Beaussoubre, and Wolfgang Fieber*

Delivery systems with low-permeability barriers and controllable release are crucial for the encapsulation of cells, pharmaceuticals, vitamins, inks, or fragrance and flavor molecules.[1] Core/shell capsules provide a stable microenvironment and protect sensitive chemicals from degradation, undesired reactions, or evaporation.[2] Traditionally, volatile oils have been encapsulated using synthetic polymers.[3] While there is a strong interest in using capsule wall materials of biological origin, their barrier properties for small-molecular-weight, highly volatile active ingredients remain inferior to those of polyurea or aminoplast capsules with walls that are produced synthetically.[1,3] Herein, we describe core/shell capsules with dense walls composed entirely of a biopolymer scaffold interpenetrated by a network of amorphous silica. We first formed a weakly acidic hydrogel shell around an oil drop. This shell then served as a scaffold to induce protein-directed mineralization of silicon dioxide from a liquid-silica precursor. The precipitation process occurring in the hydrogel scaffold consumes water and forms SiO_2, yielding dense shells with very low permeability for volatile organic compounds and adjustable mechanical characteristics.

Macroscopic biopolymer layers at the oil/water interface can be formed by a process called complex coacervation.[4] For this to occur, micrometer-sized droplets of a polymer-rich aqueous liquid (coacervates) are first formed by associative phase separation between a protein and a weakly anionic polyampholyte (Scheme 1). Unlike polyelectrolyte multilayers and precipitated complexes, coacervate phases remain in the liquid state[4] and are therefore moldable, providing a wide range of design possibilities for composite materials. If a aqueous dispersion of liquid coacervate droplets is mixed with an oil-in-water emulsion, the interfacial energy balance[5] between the three phases (oil/solvent/coacervate) causes the polymer-rich phase to deposit at the oil/solution interface. This coating process results in a composite emulsion of oil droplets contained within larger coacervate drops. The protein component of the outer coacervate droplet is then gelled, resulting in a physically cross-linked hydrogel wall. However, these traditional biopolymer shells often remain permeable and provide poor protection for the sensitive core materials even after further covalent cross-linking. Moreover, capsules made from classic hydrogels are soft and mechanically compliant, complicating controlled release, for example, upon chewing or rubbing on the skin.

Recent efforts to improve the mechanical and stability profiles of encapsulation systems has focused on the design and synthesis of composite structures and alternative wall

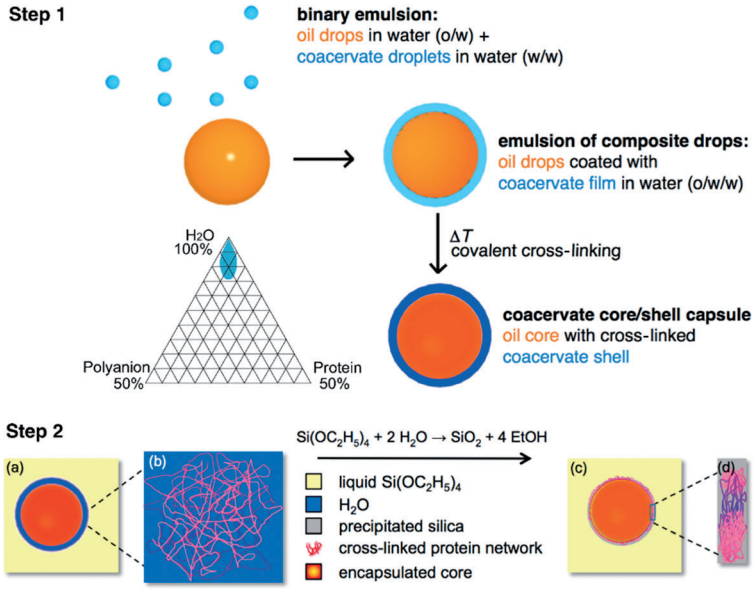

Scheme 1. The coacervate/silica scaffold-precipitation process. Step 1) Formation of scaffold capsules: complex coacervate droplets form by associative phase separation of a protein and a polyanion (the coacervation corner is indicated in the protein/polyanion/water phase diagram[4]); the coacervate droplets then deposit and coalesce around the core material (e.g. volatile oil). Physical and covalent cross-linking stabilizes the coacervate shell. Step 2) Silica formation in the coacervate shell: The capsules a) are immersed in a liquid silica precursor (TEOS). The coacervate hydrogel b) serves as a mechanical scaffold shell and provides an acidic microenvironment wherein the silica precursor locally hydrolyzes and condenses to form precipitated silica. Additionally, water consumption compresses and densifies the scaffold, resulting in composite capsules (c) with dense silica/biopolymer shells (d).

[*] Dr. P. Erni, G. Dardelle, Dr. K. Wong, P. Beaussoubre, Dr. W. Fieber
Research Division, Materials Science Department
Firmenich SA
7 Rue de la Bergère, 1217 Meyrin 2 Genève (Switzerland)
E-mail: philipp.erni@firmenich.com
M. Sillick
Research North America, Materials Science, Firmenich SA
250 Plainsboro Rd., 08536 Plainsboro Township, Princeton NJ (USA)

Supporting information for this article is available on the WWW under http://dx.doi.org/10.1002/anie.201303489.

materials, including inorganic/organic materials and silica-based hybrids.[6–15] Biomimetic silica forms in vitro in the presence of certain polypeptides and proteins found in diatoms;[16] their cell walls (known as frustules) contain vast amounts of silica and play an important role in the biogeochemical cycle of silicon.[17] These structures can be emulated with synthetic cysteine–lysine block copolypeptides.[18] Siliceous materials also form with naturally occurring amines,[19] silk proteins,[20] or polysaccharide/protein assemblies.[21] Aqueous carboxymethyl cellulose beads with alginate/aminopropyl-silane coatings have been used for enzyme encapsulation.[9] Microcapsules or hollow particles with silica walls[22] and silica-coated liposome-type containers with a hydrophilic interior[23] have been synthesized; however, the silica wall typically remains porous and permeable to small-molecular weight compounds.

Herein, we formed hybrid biopolymer/silicon oxide capsules by precipitating silica within a pre-formed coacervate hydrogel scaffold. This approach exemplifies two concepts from nature: 1) complex coacervation forms a polymer-enriched, moldable material that serves as a scaffold; 2) protein-directed silicification allows for fine-tuning of the mechanical properties. In combination, both approaches also yield an additional feature not achieved by either of the two alone, or by other composite silica materials: the resulting coacervate/silica shells have excellent barrier properties against diffusion, thereby allowing for isolation and protection of sensitive, small-molecular weight organic molecules from their environment.

We first encapsulated a hydrophobic core material in a protein/polyanion coacervate shell, followed by polymer-templated silica precipitation in the weakly acidic microenvironment provided by this coacervate hydrogel (Scheme 1). These scaffold capsules for subsequent silicification were made by complex coacervation of a protein (gelatin) with a polyanion (*Acacia* gum) and cross-linked with glutaraldehyde or transglutaminase. We separated the template capsules from the aqueous continuous phase and added them directly to pure liquid tetraethyl orthosilicate (TEOS). Upon contact with water, this alkoxide undergoes hydrolysis[10–15,24] according to the net reaction $Si(OC_2H_5)_4 + 2H_2O \rightarrow SiO_2 + 4C_2H_5OH$, resulting in solid SiO_2 by way of a series of condensation reactions with ethanol as a side product. In alkaline environments, nucleation and growth lead to colloidal silica particles.[24] In contrast, the acidic conditions used here yielded a continuous polymeric silica network. The cross-linked coacervate shell shrunk after immersion in TEOS; its thickness continued to decrease for about 90 minutes. This shrinkage during silica formation was due to the consumption of water from the coacervate as the TEOS was hydrolyzed (Figure 1). In the presence of excess liquid silica precursor, the available amount of water therefore limits silica formation. The final capsules retained their shape when dried and re-suspended in water. In dry form, they are nearly spherical beads with smooth and reflective surfaces (Figure 1). They are spherical enough to roll on flat surfaces, like marbles, and can easily be crushed, releasing the core liquid in a burst.

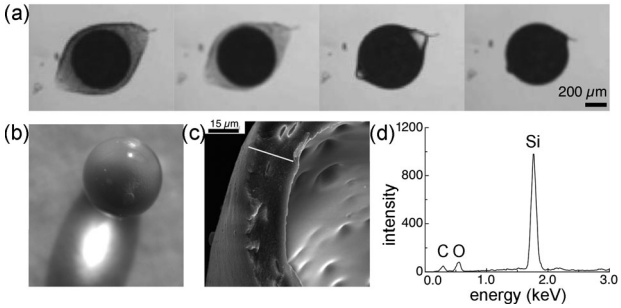

Figure 1. a,b) Silicification of a coacervate core/shell capsule (large capsule with diameter 500 μm; brightfield microscopy—the encapsulated core appears black; the gray background fluid is TEOS; over 30 min). The result (b) is a dense, composite silica/coacervate shell with reduced shell thickness but strongly improved mechanical and barrier properties. c) silicified coacervate shell (SEM micrograph; the wall has shrunken to a thickness of about 20 μm; line: EDS scan trace). d) EDS elemental scan of silicified shells.

The size distribution of the capsules can be controlled by the flow characteristics of the initial emulsification process; herein, we used a miniature stirred-tank reactor, resulting in relatively large beads (100–500 μm). However, any emulsification process yielding stable emulsions can be used, including microfluidic channels or membrane emulsification. An example of a silicified capsule containing limonene, stored for 20 months at room temperature and then crushed between microscope slides is shown in Figure 3. Rupture of the shell resulted in glass-like fragments. To avoid the formation of large, grape-like agglomerates of capsules glued together by silica bridges, we added a phospholipid-based surfactant to the continuous phase.

To confirm the presence of silica formed by in situ precipitation, we use solid-state NMR spectroscopy. The application of cross-polarization/magic-angle-spinning (CP/MAS) ^{29}Si NMR spectroscopy to silica materials has been established by Sindorf and Maciel.[25] It is an effective probe for the surface geometry, in particular of the degrees of condensation.[26] Most importantly, the method is also well-suited for structural studies on polymer/silica composites.[27] We performed measurements on silicified coacervates with dried samples of empty capsule shells. The ^{29}Si CP/MAS-NMR spectra revealed one major peak at a chemical shift of -102 ppm and two minor peaks at -92 and -112 ppm. In the melt state, silicates are 3D networks of SiO_4 tetrahedra bridged with oxygen atoms. If cation oxides are introduced, this melt structure is disrupted, and non-bridging oxygen atoms are present. A notation often used to quantify these structures uses the symbol Q to identify the Q^n species, with n indicating the number of bridging O atoms per SiO_4 tetrahedron.[28] Following El Rassy et al.,[29] we attributed the peaks shown in Figure 2 to Q^2, Q^3, and Q^4 silicon groups. Analytical integration suggested that the Q^3 tri-coordinated silicon dominates, indicating a high fraction of interfacial silanol groups, likely associated with a large internal surface area.[29] Direct comparison with reference SiO_2 confirmed that all three peaks are at virtually identical values of chemical shift, but with slightly different apparent magni-

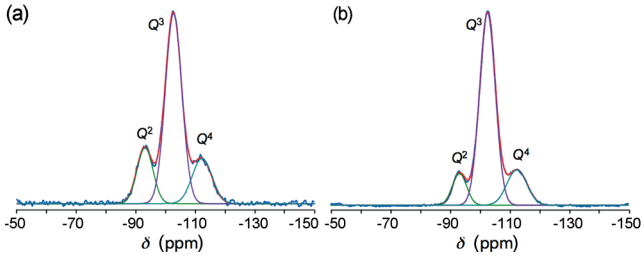

Figure 2. CP/MAS ^{29}Si NMR spectra of scaffold-precipitated silica/coacervate shells (a) compared to reference SiO_2 (b). Spectrum deconvolution reveals three distinct peaks, referred to as Q^2 (geminal silanol, green curve), Q^3 (silanol, purple curve), and Q^4 (siloxane, blue curve). Peak-wise analytical integration reveals that the maxima are at identical chemical shifts, with dominant apparent peaks for Q^3 tri-coordinated silicon.

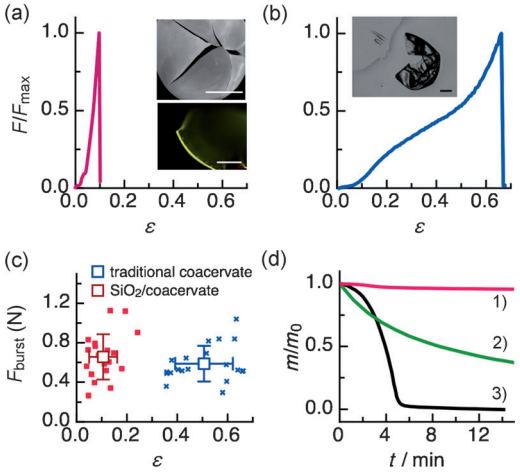

Figure 3. Mechanical properties of core/shell capsules with coacervate/silica walls and retention of an encapsulated model volatile compound, *R*-(+)-limonene. a,b) Typical force-deformation curves (F/F_{burst} is the measured force normalized by the burst force; ε is the deformation) of coacervate/silica composite capsules (a) compared to capsules with classic coacervate, polymer-only shells (b). Insets: coacervate/silica capsules fracture as rigid, brittle materials, whereas traditional, polymer-only coacervate capsules yield deflated, flexible, rubbery-type skins upon fracture; scale bars = 300 μm; a) SEM (top) and fluorescence microscopy (bottom) images; b) phase contrast image; capsule surrounded by the core liquid released upon fracture. c) Burst force versus deformation at burst plotted for ensembles of silica/coacervate and traditional coacervate-only capsules. d) Comparison with traditional silica delivery systems: retention of *R*-(+)-limonene as measured by thermogravimetry; the normalized volatile content $m(t)/m_0$ at 120 °C is shown. 1) silica/coacervate core/shell capsules; 2) traditional SiO_2 precipitated in situ around phospholipid-stabilized limonene droplets; 3) porous silica reference directly loaded with the volatile oil by capillary adsorption (see Supporting Information for details).

tudes. To further support our hypothesis that the shells consist of interpenetrating networks of cross-linked protein/polyanion coacervates and amorphously precipitated polymeric silica, we compared the specific surface areas of the shell material before and after removal of the organic coacervate component by calcination. Indeed, we found a dramatic increase in the specific surface area from $S_{spec} = 17\ m^2 g^{-1}$ for the intact, dry shells before calcination to $S_{spec} = 589\ m^2 g^{-1}$, indicating that removal of the coacervated polymer "glue" from the precipitated silica yields a highly porous material, wherein the pores are the leftovers of the organic polymer strands (see Supporting Information). Using the EDS detector of the SEM, we performed line scans along selected trajectories over the cross-section of fractured capsule shells (Figure 1). Silicon was the primary component of the shell, by far outweighing all other signals (mostly carbon and oxygen). Si was distributed evenly across the shell, and the EDS spectrum was independent of the sampling region. In view of the process and the origin of the silicon for the samples investigated herein, the EDS scan suggested that the process indeed yielded a dense, homogeneous solid shell rich in Si.

Depending on the original coacervate compositions, pH values and capsule sizes, we found the silica contents in the composite shells to be around 12–46 % *w*/*w* and mass loadings of the core material to be around 81–92 % *w*/*w*. Owing to the extremely low permeability of this composite structure, the mass loading of the active ingredient remained constant for months, and, without mechanical fracture, thermogravimetric and volatile headspace concentration measurements[30] over dry, single capsules revealed no loss of the encapsulated compounds.

The mechanical properties of the coacervate/silica core/shell capsules are shown in Figure 3 a,b and compared to traditional coacervate (polymer-only) capsules. Force-displacement curves measured in compression between parallel plates revealed that the burst force was similar for the two types of capsules, with values around 0.6 ± 0.1 N. In contrast, the apparent compressional deformation at the point of burst was significantly different: the brittle hybrid capsules burst already at a compressional deformation of $\varepsilon \approx 10\,\%$, whereas the "rubbery", polymer-only coacervate capsules only burst at deformations as high as $\varepsilon \approx 40$–$60\,\%$. The fragments of the ruptured biohybrid glass shells were pointed, with sharp edges, as is typical for spherical rigid shells after brittle fracture. In contrast, the residues of the burst traditional, polymer-only coacervate shells appeared as contiguous, deflated shells. The retention of volatile model fragrance compounds in composite SiO_2/coacervate capsules was also comparable to traditional organic/inorganic silica encapsulates (with significant loss of volatile compounds at a temperature of 120 °C; Figure 3 d, curve 2), or with standard, high-surface-area porous silica loaded with an adsorbed volatile oil (Figure 3 d, curve 3; complete loss of volatile compounds within a few minutes; see Supporting Information).

In conclusion, core/shell capsules with biohybrid glass walls were formed by precipitating amorphous silica inside a hydrogel scaffold shell. The scaffold was provided by a biopolymer coacervate and has two functions: 1) it is a shape template, molding the final shape of the composite shell; 2) it provides an acidic microenvironment to locally induce silica precipitation from a liquid silica precursor. Because amorphous silica was formed by hydrolysis of the precursor, the precipitation not only resulted in silica formation, but simultaneously consumed the water present in the coacervate, thereby densifying the shell. An outstanding feature of these silica/biopolymer composite shells is their

capacity to serve as a low-permeability barrier for small, volatile molecules. The corresponding dramatic decrease in mass transfer through the shell suggests that these core/shell structures could be an interesting alternative to encapsulation using classical porous silica precipitates,[6,31] where a drying step is typically necessary. Depending on the pore structure and tortuosity of the barrier, volatile molecules are prone to losses by evaporation. The co-continuous, silica-in-coacervate shells created herein have outstanding barrier and mechanical properties, even for encapsulation of relatively small volatile molecules. As a specific example, we encapsulated model volatile fragrance molecules for protection against evaporation and degradation and demonstrated mechanically triggered release upon fracture of the capsule shell. More generally, this method is applicable to a wide range of chemical systems provided their oil/water partition coefficients allow them to form an initial oil-in-water emulsion, alone or with an auxiliary hydrophobic solvent or dispersant.

Experimental Section

Coacervate capsule templates: We first prepared the core–shell capsules with biopolymer-based hydrogel walls. The wall material was generated by associative phase separation (complex coacervation) with a protein (gelatin standard, 200 Bloom, Weishardt, Graulhet, France) and *Acacia* gum (CNI, Rouen, France) as the polyanion, as described elsewhere.[32] Stock solutions were prepared at 10.0% *w*/*w* (adjusted for humidity present in the polymer raw materials) and kept at 50°C. Equal volumes of the two solutions were mixed and the pH value was adjusted to 4.6 with lactic acid (Fluka 69975, used as a 50% *w*/*w* aqueous solution in Millipore water). The volatile oil phase (*R*-(+)-limonene, 97%, Sigma) was then emulsified into this mixture with an impeller laboratory stirrer over 5 min to obtain an emulsion with an oil-droplet weight fraction of 25.5% *w*/*w* and number-based mean droplet size of 200–400 μm. We induced phase separation by diluting with water to give final polymer concentrations of 1.7% *w*/*w* each, thereby moving the system into the complex coacervation corner of the water/protein/polyanion phase diagram.[4] After cooling to 20°C the pH value was adjusted to 4.5 and the capsules shells were cross-linked enzymatically with transglutaminase (Ajinomoto, Japan) over 14 h at 20°C. Alternatively, glutaraldehyde can be used for covalent cross-linking. Gelatin forms physical thermoreversible networks, whereas covalent cross-linking creates a second, coexisting network locked in place by chemical bonds.[32] Micro-differential scanning calorimetry (μ-DSC) during heating/cooling cycles allows measurement of the change in the enthalpy of renaturation ΔH_r of the reversible network at varying degrees of cross-linking.[32] Reproducible cross-linking conditions are important because free amine groups are expected to play a role in the protein-directed silica precipitation, as discussed above.

In situ scaffold precipitation: The suspension of cross-linked capsules was acidified to pH 2 with a 1M hydrochloric acid solution (Sigma H9892), separated using a 150 μm mesh size filter and immediately immersed in TEOS (≥99.0% GC, Aldrich 86578) containing 0.5% *w*/*w* of a phospholipid emulsifier (Lecithin 100IP obtained from Sternchemie, Germany) to avoid aggregation. Filtered precursor capsules (20 g) and TEOS (20 g) were mixed in a beaker. The water content of the coacervate scaffold was 88.5% *w*/*w* for the examples shown here (see Supporting Information); this directly determines the possible amount of SiO_2 that can form. The resulting suspension was stirred gently for 150 min at 23°C. To monitor the process, the same procedure was performed with individual capsules in a transparent microscopy cell (Type 402.000, Hellma, Germany) filled with excess TEOS and observed by brightfield microscopy in transmission mode (see Figure 1a). Following this step, the capsules were again filtered, rinsed three times with 100 mL of a 0.05M HCl solution in a 50:50 *v*/*v* water-ethanol mixture, and dried on filter paper under a nitrogen stream.

^{29}Si solid-state MAS-NMR: Experiments were carried out at room temperature on a Bruker AV II 400 MHz spectrometer equipped with a 4 mm CP/MAS solid-state probe head. The capsule samples were broken using a mortar and pestle, washed several times with isopropanol to remove the oil core, rinsed with millipore water, and dried under vacuum. The remaining fragments were once again ground to obtain a fine powder and filled into the rotor (80–100 mg). ^{29}Si spectra were acquired at a spinning speed of 4000 Hz using a ^{1}H/^{29}Si CP pulse sequence and transformed using a 30 Hz line-broadening function. Reference measurements for comparison were performed with silica gel 60 (Millipore). Quantification of the spectra was carried out using the program Dmfit (http://www.cemhti.cnrs-orleans.fr/Dmfit/).

Further characterization: For additional experimental details preparation of traditional silica delivery systems for comparison, on electron microscopy, energy dispersive x-ray spectroscopy (EDS), mechanical measurements, thermogravimetry (TGA), and nitrogen sorption experiments see the Supporting Information.

Received: April 24, 2013
Published online: July 23, 2013

Keywords: biomineralization · core/shell capsules · coacervates · encapsulation · inorganic/organic hybrids

[1] a) D. Cui, J. Jing, T. Boudou, I. Pignot-Paintrand, S. De Koker, B. G. De Geest, C. Picart, R. Auzely-Velty, *Adv. Mater.* **2011**, *23*, H200; b) Y. Yeo, E. Bellas, W. Firestone, R. Langer, D. S. Kohane, *J. Agric. Food Chem.* **2005**, *53*, 7518; c) P. W. Chen, R. M. Erb, A. R. Studart, *Langmuir* **2012**, *28*, 144.

[2] a) C. J. Martinez, J. W. Kim, C. Ye, I. Ortiz, A. C. Rowat, M. Marquez, D. Weitz, *Macromol. Biosci.* **2012**, *12*, 946; b) W. H. Tan, S. Takeuchi, *Adv. Mater.* **2007**, *19*, 2696; c) W.-H. Tan, S. Takeuchi, *Lab Chip* **2008**, *8*, 259.

[3] M. Pretzl, M. Neubauer, M. Tekaat, C. Kunert, C. Kuttner, G. Leon, D. Berthier, P. Erni, L. Ouali, A. Fery, *ACS Appl. Mater. Interfaces* **2012**, *4*, 2940.

[4] a) C. G. de Kruif, F. Weinbreck, R. de Vries, *Curr. Opin. Colloid Interface Sci.* **2004**, *9*, 340; b) H. G. Bungenberg de Jong in *Colloid Science* (Ed.: H. R. Kruyt), Elsevier, Amsterdam, **1949**, pp. 232–258; c) B. K. Green, L. Schleicher (NCR Corp.), US 2800457, **1957**.

[5] E. Spruijt, J. Sprakel, M. A. Cohen Stuart, J. van der Gucht, *Soft Matter* **2010**, *6*, 172.

[6] a) N. K. Raman, M. T. Anderson, C. J. Brinker, *Chem. Mater.* **1996**, *8*, 1682; b) S. V. Patwardhan, S. J. Clarson, C. C. Perry, *Chem. Commun.* **2005**, 1113; c) N. Nassif, O. Bouvet, M. N. Rager, C. Roux, T. Coradin, J. Livage, *Nat. Mater.* **2002**, *1*, 42; d) M. F. Desimone et al., *ACS Appl. Mater. Interfaces* **2011**, *3*, 3831; e) M. Xu, G. M. Gratson, E. B. Duoss, R. F. Shepherd, J. A. Lewis, *Soft Matter* **2006**, *2*, 205.

[7] a) N. S. Kehr, E. A. Prasetyanto, K. Benson, B. Ergün, A. Galstyan, H.-J. Galla, *Angew. Chem.* **2013**, *125*, 1194; *Angew. Chem. Int. Ed.* **2013**, *52*, 1156; b) K. Benson, E. A. Prasetyanto, H.-J. Galla, N. S. Kehr, *Soft Matter* **2012**, *8*, 10845; c) A. Sellinger, P. M. Weiss, A. Nguyen, Y. F. Lu, R. A. Assink, W. L. Gong, C. J. Brinker, *Nature* **1998**, *394*, 256.

[8] a) M. Boissière, P. J. Meadows, R. Brayner, C. Helary, J. Livage, T. Coradin, *J. Mater. Chem.* **2006**, *16*, 1178; b) T. Coradin, S. Bah, J. Livage, *Colloids Surf. B* **2004**, *35*, 53.

[9] a) F. Kurayama, S. Suzuki, T. Oyamada, T. Furusawa, M. Sato, N. Suzuki, *J. Colloid Interface Sci.* **2010**, *349*, 70; b) F. Kurayama, S.

Suzuki, N. M. Bahadur, T. Furusawa, H. Ota, M. Sato, N. Suzuki, *J. Mater. Chem.* **2012**, *22*, 15405.
[10] B. Y. Ahn, S. I. Seok, I. C. Baek, S. I. Hong, *Chem. Commun.* **2006**, 189.
[11] H. Djojoputro, X. F. Zhou, S. Z. Qiao, L. Z. Wang, C. Z. Yu, G. Q. Lu, *J. Am. Chem. Soc.* **2006**, *128*, 6320.
[12] M. Frampton, A. Vawda, J. Fletcher, P. M. Zelisko, *Chem. Commun.* **2008**, 5544.
[13] S. H. Yang, K.-B. Lee, B. Kong, J.-H. Kim, H.-S. Kim, I. S. Choi, *Angew. Chem.* **2009**, *121*, 9324; *Angew. Chem. Int. Ed.* **2009**, *48*, 9160.
[14] T. Yokoi, T. Karouji, S. Ohta, J. N. Kondo, T. Tatsumi, *Chem. Mater.* **2010**, *22*, 3900.
[15] A. B. D. Nandiyanto, S.-G. Kim, F. Iskandar, K. Okuyama, *Microporous Mesoporous Mater.* **2009**, *120*, 447.
[16] a) R. R. Naik, P. W. Whitlock, F. R. Rodriguez, L. L. Brott, D. D. Glawe, S. J. Clarson, M. O. Stone, *Chem. Commun.* **2003**, 238; b) N. Kröger, R. Deutzmann, M. Sumper, *Science* **1999**, *286*, 1129.
[17] P. Treguer, D. M. Nelson, A. J. Van Bennekom, D. J. DeMaster, A. Leynaert, B. Queguiner, *Science* **1995**, *268*, 375.
[18] J. N. Cha, G. D. Stucky, D. C. Morse, T. J. Deming, *Nature* **2000**, *403*, 289.
[19] D. J. Belton, S. V. Patwardhan, C. C. Perry, *J. Mater. Chem.* **2005**, *15*, 4629.
[20] D. J. Belton, A. J. Mieszawska, H. A. Currie, D. L. Kaplan, C. C. Perry, *Langmuir* **2012**, *28*, 4373.
[21] C. Gautier, C. Abdoul-Aribi, N. Roux, P. J. Lopez, J. Livage, T. Coradin, *Colloids Surf. B* **2008**, *65*, 140.
[22] a) C. I. Zoldesi, A. Imhof, *Adv. Mater.* **2005**, *17*, 924; b) H. Pang, S. Zhou, L. Wu, M. Chen, G. Gu, *Colloids Surf. A* **2010**, *364*, 42; c) J. Wan, H. A. Stone, *Langmuir* **2012**, *28*, 37; d) K. Du, X. Cui, B. Tang, *Chem. Eng. Sci.* **2013**, *98*, 212.
[23] S. Bégu, A. A. Pouessel, D. A. Lerner, C. Tourné-Péteilh, J. M. Devoisselle, *J. Controlled Release* **2007**, *118*, 1.
[24] a) S. A. Khan, A. Günther, M. A. Schmidt, K. F. Jensen, *Langmuir* **2004**, *20*, 8604; b) W. Stöber, A. Fink, E. Bohn, *J. Colloid Interface Sci.* **1968**, *26*, 62.
[25] D. W. Sindorf, G. E. Maciel, *J. Am. Chem. Soc.* **1983**, *105*, 1487.
[26] E. Zendri, V. Lucchini, G. Biscontin, Z. M. Morabito, *Appl. Clay Sci.* **2004**, *25*, 1.
[27] G. K. Agarwal, J. J. Titman, M. J. Percy, S. P. Armes, *J. Phys. Chem. B* **2003**, *107*, 12497.
[28] W. J. Malfait, W. E. Halter, Y. Morizet, B. H. Meier, R. Verel, *Geochim. Cosmochim. Acta* **2007**, *71*, 6002.
[29] H. El Rassy, E. Belamie, J. Livage, T. Coradin, *Langmuir* **2005**, *21*, 8584.
[30] B. P. Binks, P. D. I. Fletcher, B. L. Holt, P. Beaussoubre, K. Wong, *Langmuir* **2010**, *26*, 18024.
[31] S. R. Veith, E. Hughes, S. E. Pratsinis, *J. Controlled Release* **2004**, *99*, 315.
[32] a) P. Erni, A. Parker, *Langmuir* **2012**, *28*, 7757; b) G. Dardelle, A. Subramaniam, V. Normand, *Soft Matter* **2011**, *7*, 3315.